Cellulose Nanocrystal/Gold Nanoparticle Composite as a Matrix for Enzyme Immobilization

Khaled A. Mahmoud, Keith B. Male, Sabahudin Hrapovic, and John H. T. Luong*

Biotechnology Research Institute, Canada National Research Council, 6100 Royalmount Avenue, Montreal, Canada H4P 2R2

ABSTRACT A novel nanocomposite consisting of cellulose nanocrystals (CNCs) functionalized with gold nanoparticles (AuNPs) serving as an excellent support for enzyme immobilization with phenomenally high loading is presented in this work. As testing models, cyclodextrin glycosyl transferase (CGTase) and alcohol oxidase were conjugated on an activated CNC/AuNP matrix. This catalytic platform exhibits significant biocatalytic activity with excellent enzyme stability and without apparent loss of the original activity. The recovered specific activities were ~70% and 95% for CGTase and alcohol oxidase, respectively. This novel and inexpensive material is anticipated to extend to other enzymes, enhancing the enzyme loading and activity as well as the stability in both operation and storage.

KEYWORDS: cellulose nanocrystals • gold nanoparticles • enzyme • CGTase • immobilization

INTRODUCTION

An ideal matrix for enzyme/protein immobilization should be biocompatible without compromising the protein structure and thereby its biological activity. The requirement for maximal enzyme loading with high activity fosters intensive research for the development of high-surface-area nanomaterials with facile bioconjugation. Cellulose nanocrystals (CNCs) have been prepared and isolated from natural cellulosic fibers by acid hydrolysis (1, 2). CNCs with different morphologies can also be obtained by varying the source of cellulose and the reaction conditions (3−6). Conjugation of CNCs with nanomaterials is expected to provide excellent hybrid supports for enzymes. Gold nanoparticles (AuNPs) can be functionalized with thiolated molecules with carboxylic groups, which, in turn, are conjugated with amine groups of the proteins (7−11). Of interest is the utilization of cyclodextrins as stabilizing agents to control the size and shape of AuNPs to preserve their finely dispersed state (12). This communication presents a novel method to covalently immobilize enzymes on a CNC/AuNP composite with significantly high enzyme loading and excellent stability.

EXPERIMENTAL SECTION

Materials. Pectate lyase-treated flax fibers were obtained from Dr. D. Rho (Biotechnology Research Institute, Canada National Research Council, Montreal, Quebec, Canada). Sodium borohydride (SBH), gold(III) chloride trihydrate, sodium phosphate mono- and dibasic, 2-(*N*-morpholino)ethanesulfonic acid (MES), 1-ethyl-3-[3-(dimethylamino)propyl]carbodiimide (EDC), *N*-hydroxysulfosuccinimide (NHS), and α-cyclodextrin (α-CD) were purchased from Sigma-Aldrich. ACS-grade H_2SO_4, HNO_3, and H_2O_2 (35%) were used without further purification. Alcohol oxidase (*Pichia pastoria*, 39 U/mg and 34 mg/mL) and cyclodextrin glycosyl transferase (CGTase) were obtained from Sigma-Aldrich and Amano Enzyme Inc. (2-7, 1-Chome, Nishiki, Naka-ku, Nagoya 460-8630, Japan), respectively.

Preparation of CNCs. CNCs were prepared from enzyme-treated flax fibers by a modified acid hydrolysis procedure. In brief, flax fibers were ground through a 20-mesh screen down to 0.85 mm fiber size. The resulting flax fibers (0.5 g) were stirred in 20 mL of an acid mixture (3:1 65% H_2SO_4/65% HNO_3), and 10 mL of H_2O_2 was added dropwise. (**Caution!** *Sulfuric acid reacts with H_2O_2 to release heat; thus, the reaction should be handled in the fume hood with precaution and proper safety protection.*). The temperature was brought to 45 °C and the reaction continued for 3 h. After a 10-fold dilution with deionized water to terminate the reaction, the suspension was centrifuged at 10 000 rpm, followed by washing until the pH was ~6. The sample was then dialyzed against distilled water for 3 days. A mixed-bed ion-exchange resin (DOWEX MR-3) was added to the CNC suspension, allowed to stand for 2 days, and removed by filtration (Whatman 541). The colloidal solution was concentrated to ~23 mg/mL and sonicated for 35 min at room temperature.

Preparation and Surface Modification of the CNC/AuNP Conjugate. AuNPs were deposited on CNC by the reduction of gold(III) chloride trihydrate by SBH in the presence of the CNC colloid according to the method of Birrell et al. (13) with modifications. In brief, $HAuCl_4 \cdot 3H_2O$ (10 mM, 1.6 mL) and α-CD (2 mM, 2 mL) were added to 4 mL (23 mg/mL) of CNC, and then 20 μL aliquots of freshly prepared ice-cold 0.1 M SBH ($NaBH_4$) were added to the slowly mixing solution of Au salt/CNC until a stable reddish colloid was observed (100 μL of $NaBH_4$). The solution was left for 24 h at 22 °C to stabilize. The AuNP-labeled CNC was washed and centrifuged at 10 000 rpm three times to remove the unbound AuNPs. The supernatant was clear after the first washing cycle. The particle size was determined from UV−vis spectroscopy and confirmed by transmission electron microscopy (TEM). The CNC/AuNP colloid was centrifuged, and the pellet was resuspended in pure ethanol.

* Correcponding author. Fax: (+1) 514 496 6265. E-mail: john.luong@cnrc-nrc.gc.ca or j.luong@ucc.ie.
Received for review May 15, 2009 and accepted June 30, 2009

DOI: 10.1021/am900331d

This step was repeated three times. The resulting CNC/AuNP colloid was incubated in a 0.05 M ethanol solution of thioctic acid (Thc) for 24 h. Thc was thus covalently attached to AuNP through Au−S bond formation.

Carbodiimide Coupling of Enzymes. Grafting of CGTase and alcohol oxidase onto the CNC/AuNP surface was performed using the well-established two-step carbodiimide coupling protocol. First, carboxylic acid groups of Thc bound to AuNPs were activated. EDC and NHS stock solutions were prepared in 0.05 M MES and 0.5 M NaCl buffer, pH 5.7. CNC/AuNP/Thc (12 mg/mL) was resuspended in 0.05 M MES and 0.5 M NaCl buffer, pH 5.7 (5 mL), prior to the addition of EDC. A carboxylated CNC suspension (0.5 mL) was stirred with 5 and 10 mM EDC and NHS in MES buffer, respectively, for 30 min at room temperature. The NHS activation was confirmed by FTIR spectroscopy upon analysis of freeze-dried CNCs. Excess reactants were removed from the EDC-activated CNCs by successive centrifugation and dilution with deionized water, followed by filtering and concentration with a MicroKross ultrafilter (MWCO 50 kD). The activated CNC/AuNP (0.5 mL, 6 mg) was transferred to a vial containing purified CGTase (~7−8 mg/mL) in a 0.1 M phosphate buffer with 0.5 M NaCl at pH 7.2. The reaction was carried out at room temperature for 2 h. CGTase (ranging from 0.08 to 2.8 mg) was added to determine the maximum binding capacity of the modified CNC. After the reaction, the samples were centrifuged and the supernatants were collected. After extensive washing, the CNC pellets were resuspended in 500 μL of 0.1 M phosphate buffer and 0.5 M NaCl, pH 7.2, and were assessed along with the supernatants for the enzyme activity and their protein content.

Characterization. A Hitachi field-emission gun scanning electron microscope (FEG-SEM; model S-4700, Tokyo, Japan) was used for the analysis of CNC/AuNPs. The FEG-SEM was equipped with an energy-dispersive X-ray (EDX) spectrometer. The FEG-SEM/EDX system was operated in high-vacuum mode at 15 kV, with an emission current of 21.5 μA and a working distance of 12 mm. The EDX has software with a database of reference spectra for elemental analysis, compositional nanoanalysis, and mapping. A drop of nanomaterial was dried on a silica plate and introduced into the chamber. TEM micrographs were obtained by a Hitachi (model H-7500, Tokyo, Japan) transmission electron microscope at 60 and 80 kV. A small amount of sample was suspended in methanol and sonicated to disperse the material. A 20 μL drop of a well-dispersed suspension was then dried on a Formvar carbon-coated grid and analyzed. Atomic force microscopy (AFM) imaging was carried out by a Nanoscope IV system (Veeco Digital Instruments, Santa Barbara, CA), operating in tapping mode. Silicon AFM probes with a cantilever length of 125 mm and drive frequencies of 235−255 kHz were used for imaging. The imaging scan speed was 0.50 Hz at 512 lines/scan. All height measurements and size distributions were calculated from the software provided with the instrument.

RESULTS AND DISCUSSION

The off-white CNC suspension was extracted from flax fibers by a modified acid hydrolysis method, using a new acid composition [3:1:2 65% H_2SO_4/65% HNO_3/35% H_2O_2], as described in the Experimental Section. A combination of the two acids with H_2O_2 allows for in situ purification and bleaching of the enzyme-treated fibers during the preparation of CNC. Notice that in the presence of the acid mixture, together with H_2O_2, a small portion of the surface C_6 primary hydroxyls of CNC was oxidized to carboxylic acid groups, as confirmed by an IR peak at ~1730 cm^{-1} (Figure S2a in the Supporting Information). This could provide a hydrophilic surface to facilitate the subsequent functionalization

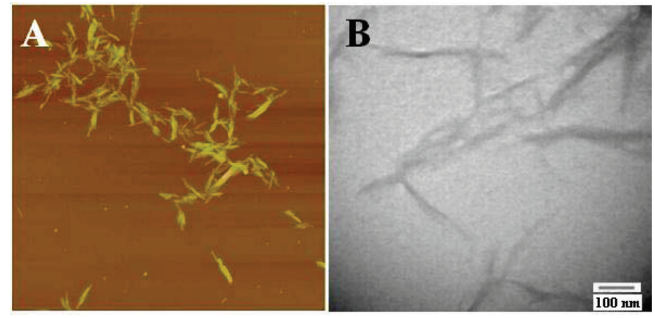

FIGURE 1. AFM (A) and TEM (B) images of CNCs. AFM scan size: 5 μm.

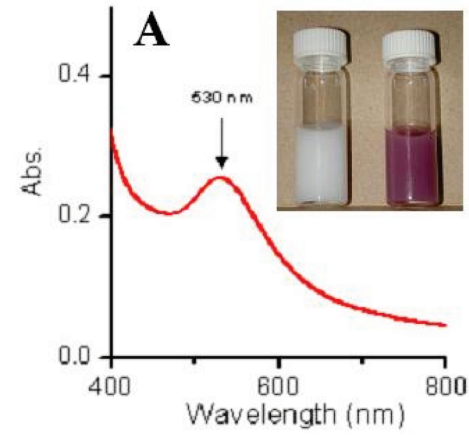

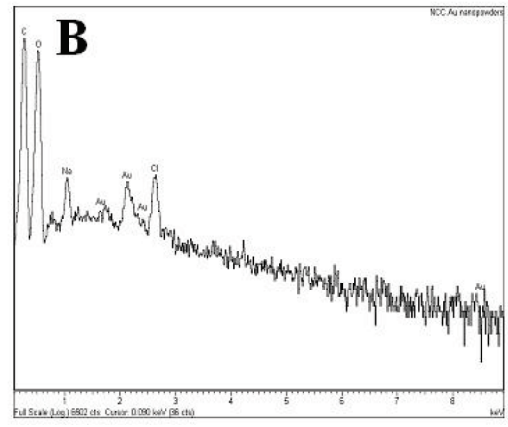

FIGURE 2. (A) UV−vis absorption spectra of an aqueous suspension of CNC/AuNP. Inset: CNCs (white) and CNC/AuNP (purple-red) (0.1 wt %). (B) EDX spectrum of a CNC/AuNP film.

steps of inorganic materials including AuNPs. The preparation produced individual and aggregated rodlike crystalline cellulose fragments, ranging from 10 to 20 nm in diameter and with a corresponding length of about 120−300 nm (Figure 1A,B).

The introduction of AuNPs was attempted to increase the surface area of CNC, aiming for a high binding efficiency with enzymes. AuNPs were deposited on the CNC by the reduction of gold(III) chloride trihydrate by SBH in the presence of α-CD as a stabilizing reagent, an adaptation of the method of Birrell et al. (13). Figure 2A compares the CNC suspension before and after the deposition of AuNPs. The AuNP/CNC suspension exhibited a red/burgundy color with

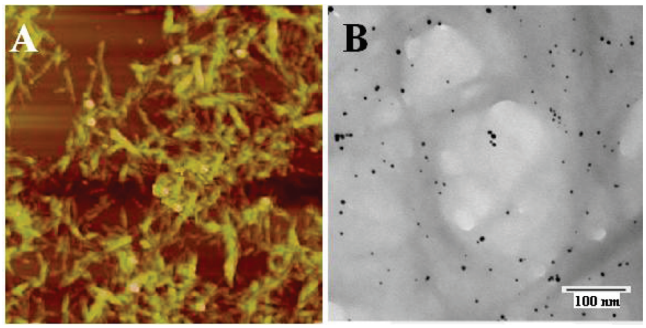

FIGURE 3. (A) AFM of CNC/AuNP. Scan size: 5 μm. (B) TEM of CNC/AuNP.

an initial absorbance of ~530 nm, known as the surface plasmon resonance peak. Figure 2B illustrates a representative EDX spectrum from the same sample as that used to collect the TEM image. The characteristic gold peaks at 2.12 and 8.49 keV were confirmed, whereas other peaks were attributed to CNC and the supporting copper grid. The AFM study (Figure 3A) displays a CNC/AuNP matrix without clearly revealing the AuNPs. However, the TEM analysis (Figure 3B) confirmed that well-distributed, spherical AuNPs (2−7 nm in diameter) were deposited on the surface of CNC. The EDX analysis of the gold nanoparticles very closely matched the starting molecular composition (Figure 3B). This observation indicated that the metal ions quantitatively were deposited onto the CNC surface (hydroxyl groups), followed by reduction with SBH to form the corresponding nanoparticles. The atomic percentage of gold was estimated from EDX of nanoparticles to be 100% of the starting gold salt. This was supported by UV−vis spectra of supernatants recovered after centrifugation. No metal ion was detected in the supernatant when the starting SBH/Au^{III} ratio was 1:1. The gold salt concentration in the reaction mixture, as well as the solution pH, played a very important role in the stabilization of the AuNP/CNC matrix. The optimal ratio of SBH/gold salt was determined to be 1:1 or less, providing an excess of gold salt in the reaction. The final pH of the solution was ~2.5−3.0. At 1.25:1 or higher, no AuNPs were observed on the CNC surface and the final solution pH was above 4.5, indicating the unstable formation of AuNP/CNC. These findings are in contrast to the standard protocols for forming AuNPs, whereby SBH had to be in a 5−10-fold excess over the gold salt and the gold salt concentration was lower than 1 mM, in order to prevent the aggregation of AuNPs (13). Therefore, CNC allowed for high AuNP loading onto CNC as well as provided facile stabilization of AuNPs.

CGTase could be an important test model for immobilization on the functionalized CNC/AuNP platform. This enzyme plays an important role in the starch industry for the production of cyclodextrins. Immobilized CGTase has been widely used for the production of oligosaccharides, which allows for its reuse (14), as well as simplification of the product purification process and scale-up (15). Different methods have been applied for the immobilization of CGTase, including physical adsorption (16), entrapment (17) or covalent binding (15, 18). Immobilization by physical adsorption or entrapment provides unstable platforms due to enzyme leakage from the support matrix during the reaction (19). However, this has been attributed to the complex 3D structure of CGTase and its mechanism. The idea is to investigate whether the immobilization of CGTase (from *Bacillus macerans*) by covalent attachment to CNC/AuNP will improve the stability and maintain the catalytic activity. The molecular weight of the enzyme was ~68 kDa (Figure S1 in the Supporting Information). The purified sample (7−8 mL) had a protein concentration of 7−8 mg/mL. The enzyme covalently attached to CNC/AuNP was further assessed for its catalytic activity.

Carboxylic acid groups were introduced to the CNC/AuNP surface by coupling Thc with the AuNP surface via Au−S bonding (20, 21), followed by NHS/EDC activation at pH 5.7 (see the Supporting Information). CGTase was able to covalently bind to the activated CNC/AuNP matrix by nucleophilic attacks of amino groups on COONHS. The presence of CGTase on the support matrix was confirmed by attenuated total reflectance Fourier transform infrared measurement after immediately freeze-drying the samples to avoid possible degradation. Figure S2 in the Supporting Information shows carbonyl groups on cellulose chains with intramolecular hydrogen-bonding patterns in a frequency range between 1650 and 1670 cm^{-1} (22). An additional carbonyl peak was observed at 1730 cm^{-1} because of the carboxyl group on the CNC surface (Figure S2b in the Supporting Information). This feature disappeared after EDC/NHS activation of carboxylated CNC, followed by the coupling of CGTase (Figure S2c in the Supporting Information). In the absorption spectrum of enzyme-grafted CNC/AuNP, a strong absorption band at ~3340 cm^{-1} was assigned for protein NHs, a shoulder at 1716 cm^{-1} represented the C═O stretching, and a carbonyl peak at 1650 cm^{-1} was assigned for the amide linkage between the enzyme and CNC/AuNP (Figure S2c in the Supporting Information). EDX analysis also confirmed the enzyme attachment on the CNC/AuNP matrix, as reflected by an additional intense sulfur peak arising from thiol-containing amino acid residues within the enzyme domain (Figure S3 in the Supporting Information).

The AuNP-modified CNC possessed a CGTase binding capacity of 165 mg/g of CNC, as shown in Figure 4A. The total protein, recovered from the supernatants and pellets for each amount tested, was ~100%. Less than 10% CGTase activity was detected in the supernatants at low enzyme loading (<25 000 U/g of CNC). At this enzyme loading, most of the activity (>90%) was associated with the CNC pellets such that the total recovery of the activity was close to 100%, compared to 70% or less on other supports (23, 24). As the enzyme loading was increased (>25 000 U/g of CNC), the total activity recovered from the supernatants and pellets ranged from 67 to 82%. The maximum CGTase binding activity leveled off at ~50 000 U/g of CNC, as shown in Figure 4B. Our method provided a significant improvement in the specific enzyme activity compared with previous studies on the covalent immobilization of CGTase (25, 27).

The specific activity of the bound CGTase was ~300 U/mg of protein, which represents close to 70% of the specific

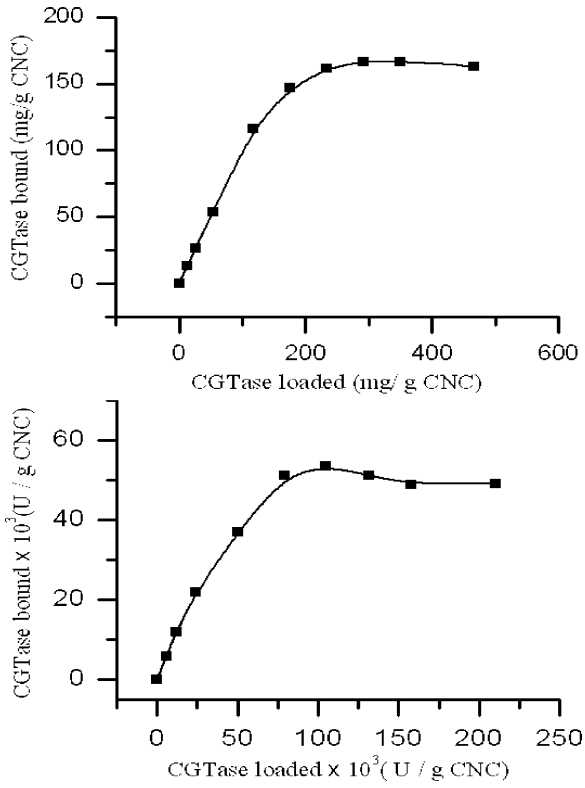

FIGURE 4. Effect of the CGTase loading onto a CNC/AuNP support of (A, top) protein binding (±5%) and (B, bottom) biocatalytic activity (±7%).

activity (450 U/mg) of the purified CGTase. The remarkable improvement of enzyme loading in our work, compared to other existing enzyme carriers, could be attributed to the higher exposed surface area provided by the CNC/AuNP matrix. Despite extensive washing of the pellets, no significant leaking of CGTase from the CNC support matrix was observed. To evaluate the reliability of this protocol, the same procedure was also used to immobilize alcohol oxidase, an enzyme that catalyzes the oxidation of lower primary aliphatic alcohols with oxygen as the electron acceptor, on the CNC/AuNP support, followed by assay of the catalytic activities for both immobilized and free alcohol oxidase. Similar behavior was observed where the specific activity of the bound alcohol oxidase was ~ 37 U/mg of protein or ~95% of the specific enzyme activity (39 U/mg; Figure S4 in the Supporting Information).

The unique assembly of AuNPs bound to CNCs enables the construction of an excellent support for the immobilization of enzymes. As a testing model, CGTase conjugated on the CNC/AuNP matrix exhibits significant biocatalytic activity. This novel proof of concept provides a platform that could be widely adapted for the scale-up of enzyme-catalyzed processes at the industrial level with improved homogeneity, reusability, and cost effectiveness. This novel and inexpensive material is anticipated to extend to other enzymes to enhance the activity, enzyme loading, and stability in both operation and storage. The enzymatic properties of immobilized CGTase and others are being investigated in detail in our laboratories and compared with those of the soluble enzymes.

Acknowledgment. The authors thank Prof. S. Omanovic of the Department of Chemical Engineering, McGill University, Montreal, Quebec, Canada, for FTIR measurement, E. Majid and Y. Liu of the Biotechnology Research Institute (BRI), National Research Council (NRC), Montreal, Canada, for providing AFM data, and M. Lafrance and S. St. Arnaud of BRI (NRC, Montreal, Canada) for electrophoresis studies.

Supporting Information Available: Protein and activity assays of CGTase and alcohol oxidase enzymes, FTIR and EDX of immobilized CGTase on an activated CNC/AuNP film, and biocatalytic activity of supported alcohol oxidase on CNC/AuNP. This material is available free of charge via the Internet at http://pubs.acs.org.

REFERENCES AND NOTES

(1) Beck-Candanedo, S.; Roman, M.; Gray, D. G. *Biomacromolecules* **2005**, *6*, 1048–1054.
(2) Edgar, C. D.; Gray, D. G. *Cellulose* **2003**, *10*, 299–306.
(3) Revol, J.-F.; Godbout, L.; Dong, X.-M.; Gray, D. G.; Chanzy, H.; Maret, G. *Liq. Cryst.* **1994**, *16*, 127–134.
(4) Favier, V.; Chanzy, H.; Cavaille, J. Y. *Macromolecules* **1995**, *28*, 6365–6367.
(5) Tokoh, C.; Takabe, K.; Fujita, M.; Saiki, H. *Cellulose* **1998**, *5*, 249–261.
(6) Revol, J.-F.; Bradford, H.; Giasson, J.; Marchessault, R. H.; Gray, D. G. *Int. J. Biol. Macromol.* **1992**, *14*, 170–172.
(7) Chen, X.; Li, J.; Li, X.; Jiang, L. *Biochem. Biophys. Res. Commun.* **1998**, *245*, 352–355.
(8) Xiao, Y.; Ju, H.; Chen, H. *Anal. Chim. Acta* **1999**, *391*, 73–82.
(9) Vertegel, A. A.; Siegel, R. W.; Dordick, J. S. *Langmuir* **2004**, *20*, 6800–6807.
(10) Demers, L. M.; Mirkin, C. A.; Mucic, R. C.; Reynolds, R. A.; Leitsinger, R. L.; Viswanadham, G. *Anal. Chem.* **2000**, *72*, 5535–5541.
(11) Jun, L.; Zhou, W.; Kumbhar, J.; Wiemann, J.; Fang, J.; Carpentier, E. E.; O'Connor, C. J. *J. Solid State Chem.* **2001**, *159*, 26–31.
(12) Male, K. B.; Li, J.; Bun, C. C.; Ng, S.-C.; Luong, J. H. T. *J. Phys. Chem. C* **2008**, *112*, 443–451.
(13) Birrell, G. B.; Hedberg, K. K.; Griffith, O. H. *J. Histochem. Cytochem.* **1987**, *35*, 843–853.
(14) Plou, F. J.; Martin, M. T.; Gomez de Segura, A.; Alcalde, M.; Ballesteros, A. *Can. J. Chem.* **2002**, *80*, 743–752.
(15) Abdel-Naby, M. *Process Biochem.* **1999**, *34*, 399–405.
(16) Kim, P. S.; Shin, H. D.; Park, J. K.; Lee, Y. H. *Biotechnol. Bioprocess.* **2000**, *5*, 174–180.
(17) Lee, S. H.; Shin, H. D.; Lee, Y. H. *J. Microbiol. Biotechnol.* **1991**, *1*, 54–62.
(18) Tardioli, P. W.; Zanin, G. M.; Moraes, F. F. *Appl. Biochem. Biotechnol.* **2000**, *84*, 1003–1019.
(19) Yang, C. P.; Yu, C. S. *J. Chem. Technol. Biotechnol.* **1989**, *46*, 283–294.
(20) Biebuyck, H. A.; Bian, C. D.; Whitesides, G. M. *Langmuir* **1994**, *10*, 1825–1831.
(21) Willey, T. M.; Vance, A. L.; Bostedt, C.; van Buuren, T.; Meulenberg, R. W.; Terminello, L. J.; Fadley, C. S. *Langmuir* **2004**, *20*, 4939–4944.
(22) Prestsch, E.; Buhlmann, P.; Affolter, C. *Structural Determinationof Organic Compounds, Tables of Spectral Data*; Springer: New York, 2000.
(23) Tardioli, P. W.; Zanin, G. M.; Morae, F. F. *Enzyme Microb. Technol.* **2006**, *39*, 1270–1278.
(24) Ferrarotti, S. A.; Bolivar, J. M.; Mateo, C.; Wilson, L.; Guisan, J. M.; Fernandez-Lafuente, R. *Biotechnol. Prog.* **2006**, *22*, 1140–1145.
(25) Martin, M. T.; Plou, F. J.; Alcalde, M.; Ballesteros, A. *J. Mol. Catal. B: Enzym.* **2003**, *21*, 299–308.
(26) Amud, A. E.; da Silva, G. R. P.; Tardioli, P. W.; Soares, C. M. F.; Moraes, F. F.; Zanin, G. M. *Appl. Biochem. Biotechnol.* **2008**, *146*, 189–201.
(27) Mateo, C.; Palomo, J. M.; Fernandez-Lorente, G.; Guisan, J. M.; Fernandez-Lafuente, R. *Enzyme Microb. Technol.* **2007**, *40*, 1451–1463.

AM900331D